



Expanding the genetic spectrum of achromatopsia: novel *CNGA3* and *CNGB3* variants

Zehra Manav Yigit · Nurdamla Sandal Filikci ·
Erol Erkan · Gozde Sahin Vural ·
Mehmet Altay Unal · Evren Gumus

Received: 12 April 2025 / Accepted: 28 June 2025
© The Author(s), under exclusive licence to Springer Nature B.V. 2025

Abstract

Purpose Achromatopsia is a rare autosomal recessive disorder characterised by congenital pendular nystagmus, photophobia, decreased visual acuity, and impaired colour vision. Variants in the *CNGA3* (Achromatopsia 2, MIM#216900) and *CNGB3* (Achromatopsia 3, MIM#262300) genes account for the majority (more than 2/3) of cases, but genotype–phenotype correlations remain incompletely understood.

Methods This study aims to expand the clinical and genetic spectrum of achromatopsia by analysing five patients from three families, including two novel variants in the *CNGA3* and *CNGB3*. Comprehensive ophthalmological and genetic evaluations were performed, including best corrected visual acuity, electroretinography, optical coherence tomography, and clinical exome sequencing. Segregation analysis was conducted to confirm the inheritance pattern.

Results We identified a novel missense variant in *CNGA3* (c.1710C>A p.(Ser570Arg)) and a novel frameshift variant in *CNGB3* (c.739_754del p.(Ala247Thrfs*27)).

Conclusion Molecular dynamics simulations suggest that the *CNGA3* c.1710C>A p.(Ser570Arg) variant may act as a gain-of-function variant, leading to altered cyclic nucleotide-gated channel activity in cone photoreceptors. This finding provides new insights into the functional consequences of *CNGA3* variants in the pathophysiology of achromatopsia. Our findings provide new insights into genotype–phenotype correlations in achromatopsia and highlight the importance of early genetic diagnosis in improving disease management and genetic counselling. The identification of novel variants enhances our understanding of the genetic basis of achromatopsia and highlights the clinical utility of next-generation sequencing in the diagnosing of inherited retinal diseases.

Supplementary Information The online version contains supplementary material available at <https://doi.org/10.1007/s10792-025-03650-y>.

Z. Manav Yigit · N. Sandal Filikci
Medical Genetics Department, Medical School, Aydin
Adnan Menderes University, Zafer, 09010 Aydin, Turkey
e-mail: zehra.manav@adu.edu.tr

E. Erkan
Ophthalmology Department, Medical School, Aydin
Adnan Menderes University, Aydin, Turkey

G. Sahin Vural
Ophthalmology Department, Medical School, Balikesir
University, Balikesir, Turkey

M. A. Unal
Stem Cell Institute, Ankara University, Ankara, Turkey

E. Gumus
Medical Genetics Department, Medical School, Mugla
Sitki Kocman University, Mugla, Turkey

Keywords *CNGB3* · *CNGA3* · Achromatopsia · Novel variant · Gain of function · Genetic

Introduction

The human retina contains four types of photoreceptors: short-wavelength (blue), medium-wavelength (green), and long-wavelength (red) cones, as well as rods. Achromatopsia (rod monochromatism) is a rare congenital disorder with an autosomal recessive inheritance pattern that typically affects all three types of cone photoreceptors, with symptoms emerging within the first few months of life [1, 2].

Achromatopsia is a phenotypically and genetically heterogeneous disorder associated with pathogenic variants in six genes. Considering the 10–25% rate of cases in which the genetic aetiology has not been elucidated despite the clinical diagnosis, this number is expected to increase over the years [3]. Five of these genes (*CNGA3*, *CNGB3*, *PDE6C*, *PDE6H*, and *GNAT2*) are involved in cGMP-mediated cone phototransduction, while one (*ATF6*) encodes a protein that regulates the unfolded protein response in the endoplasmic reticulum and play a role in cone photoreceptor development [4–8]. Cyclic nucleotide-gated (CNG) channels, which belong to the voltage-gated ion channel superfamily, are found in various neuronal structures, including cone photoreceptors, olfactory sensory neurons, and the pineal gland. Variants in *CNGA3* and *CNGB3*, which encode the alpha and beta subunits of CNG channels, are the most common cause of achromatopsia, accounting for approximately 90% of cases [9, 10].

Typical symptoms of achromatopsia include reduced visual acuity, photophobia (increased sensitivity to light), and difficulty seeing in bright environments. Patients often present with high frequency, low amplitude pendular nystagmus characterised by semi-sinusoidal ocular oscillations, as well as central scotoma, eccentric fixation, and reduced or complete loss of colour discrimination [1, 11, 12]. Refractive errors are also often associated. Although no clear genotype–phenotype correlation has been established, it has been suggested that there may be phenotypic differences depending on the gene involved. In addition, paradoxical pupillary constriction (Flynn's phenomenon) may occur when patients move from a bright to a dark environment [13]. Achromatopsia was

once considered a stable condition, but recent optical coherence tomography (OCT) imaging and long-term follow-up suggest possible progressive morphological changes [14, 15].

Our study aimed to broaden the clinical and genetic spectrum of achromatopsia by analysing five cases from three families, including two novel variants.

Materials and methods

All subjects underwent a comprehensive physical and ophthalmological examination and informed consent was obtained for publication of clinical and research results.

The ophthalmic examination included measurement of best corrected visual acuity (BCVA), fundus examination after pupil dilation, spectral domain optical coherence tomography (SD-OCT), fluorescein angiography (FA), full-field electroretinography (ff-ERG) and flash visual evoked potentials (VEPs). The Metrovision multifocal ERG MonPackOne System (Metrovision, Perenches, France) was used for the ff-ERG according to ISCEV standards. Fundus autofluorescence (FAF) imaging was performed with a confocal scanning laser ophthalmoscope. Argon blue laser (HRA classic) or optically pumped solid-state laser (HRA II) with a wavelength of 488 nm was preferred as the stimulus. A barrier filter was used to ensure that absorbed light at wavelengths above 500 nm was detected. The resulting digital images were processed using a flexible frame processor and projected onto a computer screen. During FAF imaging, focusing was performed in the red free reflection mode ($\lambda=514$ nm for HRA classic, $\lambda=488$ nm for HRA II), followed by a series of images at a wavelength of 488 nm. An average image was obtained from these images to improve the signal-to-noise ratio after automatic alignment using image analysis software.

For genetic studies, exome sequencing was performed on an Illumina NextSeq sequencer using the Sophia Genetics Clinical Exome Solution V3 Kit for two patients and the Sophia Genetics Clinical Exome Solution V2 Kit for three patients. Leukocyte-derived genomic DNA was obtained from the patients' peripheral blood using the GeneAll ExgeneTM Blood DNA SV Mini Kit. Data analysis was performed using the Sophia DDM V4

analysis platform. Using genomic DNA, all exons, untranslated regions (UTRs) and variable splice site regions of the genes of interest were sequenced using standard methods and aligned to reference sequences in the human genome. Screened variants were filtered according to 1% allele frequency in population databases including dbSNP142, Human Reference Genome, 1000 Genomes Project, OMIM database, etc. and an internal database containing exomes of 3541 individuals of Turkish origin. Pathogenicity prediction was evaluated using software such as Franklin and VarSome. Sequence variant classification was based on the recommendations of

American College of Medical Genetics and Genomics (ACMG) [16]. Segregation analysis was performed to determine the carrier status of the parents of all cases.

Results

Family 1

Case 1 (C1) A 9-year-old boy, born to healthy, non-consanguineous parents of Turkish origin, was first seen at a health centre at 3 months of age because of

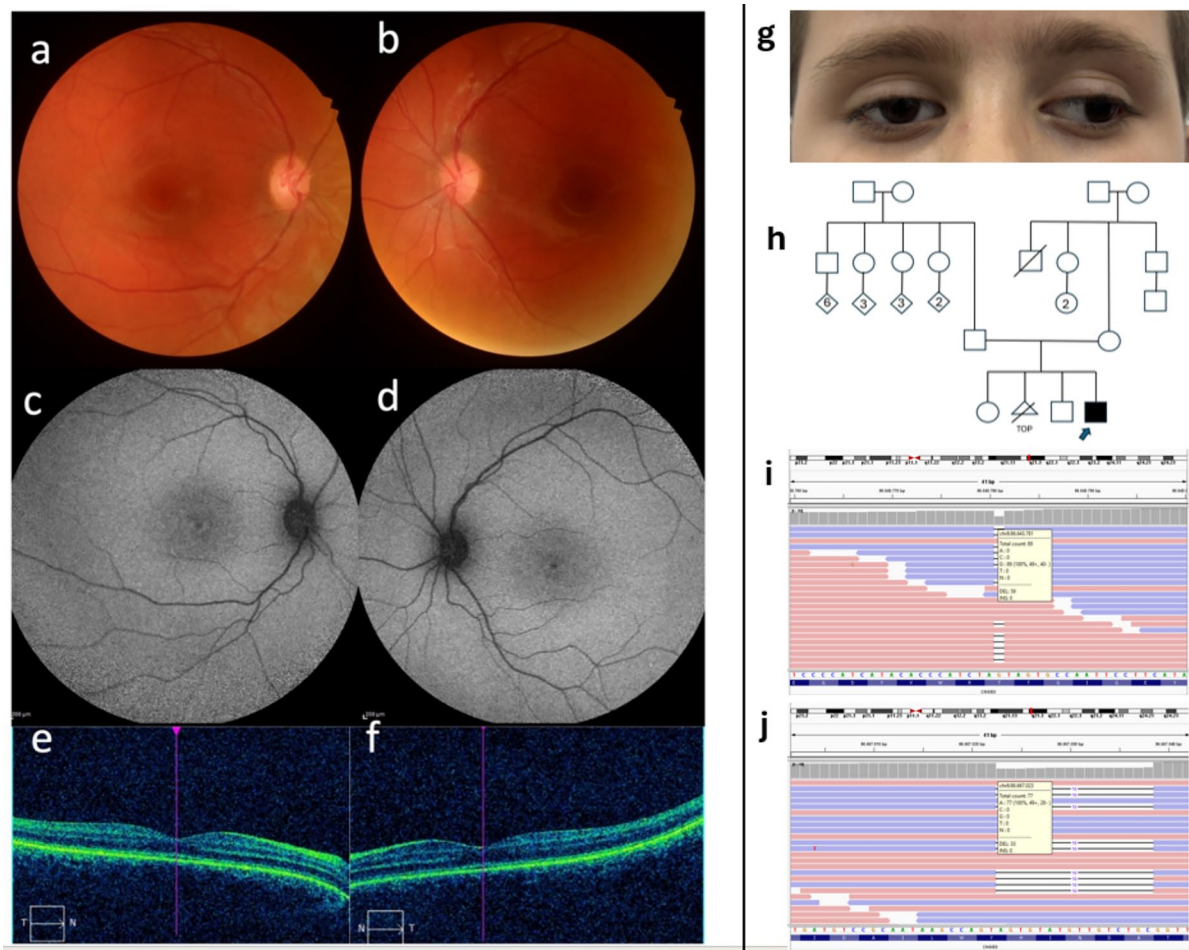


Fig. 1 **a** and **b** Bilateral optic disc pallor and arteriolar attenuation, **c** and **d** Bilateral hyperautofluorescence representing possible photoreceptor attenuation, **e** and **f** Macular OCT scans showing diffuse retinal thinning, **g** Case 1: Difficulty fully opening the eye due to photophobia and strabismus in the left eye **h** Pedigree of case 1, **i** Integrated Genomics Viewer (IGV) representation of the heterozygous *CNGB3* c.1148del p.(Thr383Ilefs*13) variant, **j** Integrated Genomics Viewer (IGV) representation of the heterozygous *CNGB3* c.739_754del p.(Ala247Thrfs*27) variant

mus in the left eye **h** Pedigree of case 1, **i** Integrated Genomics Viewer (IGV) representation of the heterozygous *CNGB3* c.1148del p.(Thr383Ilefs*13) variant, **j** Integrated Genomics Viewer (IGV) representation of the heterozygous *CNGB3* c.739_754del p.(Ala247Thrfs*27) variant

nystagmus, noticed by his mother had noticed during the neonatal period (Fig. 1). The nystagmus was present in all directions of gaze, and cranial MRI and hearing tests showed no abnormalities. Over time, the patient had difficulty seeing in daylight and was unable to walk in bright light. The family reported that his symptoms improved in dimly lit environments. Notably, he did not experience night blindness (nyctalopia). The patient was diagnosed with hypermetropia, strabismus, photophobia, and nystagmus, although he reported no significant difficulties with color discrimination. His mental development and school performance were normal.

Ocular findings Best corrected visual acuity was 20/125 bilaterally. Colour vision testing with Ishihara plates showed abnormal colour discrimination. He scored 1/21 on the Ishihara test in each eye. Slit-lamp examination of the anterior segment revealed no pathological findings. Fundus examination revealed optic disc pallor, arteriolar attenuation and bone spicules peripheral to major vascular arcs (Fig. 1a-d). OCT macular scans showed bilateral diffuse retinal thinning with no evidence of subretinal or intraretinal fluid. (Fig. 1e, f). VEP showed latency delays in both anterior visual pathways. Electroretinogram (ERG) findings indicated cone dysfunction with partial rod involvement (Table 1).

Genetic analysis identified two heterozygous variants in the *CNGB3* gene: NM_019098.5: c.1148del p.(Thr383Ilefs*13) and c.739_754del p.(Ala247Thrfs*27) (PQ874176). Parental segregation analysis confirmed that these variants were present in a compound heterozygous state (Fig. 1i, j), (Table 2).

Family 2

Case 2 (C2) The 18-year-old girl was the first child of healthy Turkish parents from the same settlement, with no reported consanguinity (Fig. 2i, l). Her family noticed bilateral nystagmus at birth, but the first examination was performed at the age of 6–7 months. According to the family, the severity of the nystagmus decreased after the age of 10 years. Since childhood, the patient has had difficulty seeing in bright light, impaired distance vision, and challenges with colour discrimination. Her developmental milestones progressed appropriately for her age.

Ocular Findings The patient presented with reduced visual acuity and oscillatory movements in both eyes. Her best corrected visual acuity was 20/125 bilaterally. Colour vision testing with Ishihara plates revealed abnormal colour discrimination. She scored 1/21 on the Ishihara test in each eye. Refractive examination revealed myopia and astigmatism in both eyes. Using the prism and cover test at distance, she had 25 prism diopters (PD) of exotropia in the primary position in the left eye. Horizontal pendular nystagmus was present bilaterally. Slit-lamp examination of the anterior segment revealed no pathological findings. Fundus examination revealed pallor of the optic disc and salt-pepper appearance in both the macula and peripheral retina. OCT macular scans showed bilateral diffuse retinal thinning with no evidence of subretinal or intraretinal fluid (Fig. 2g, h). VEP showed normal responses in both anterior visual pathways. ERG showed cone dysfunction with partial rod involvement (Table 1).

Case 3 (C3) She is the 15-year-old sister of C2 (Fig. 2k). Her family noticed bilateral nystagmus at birth, the severity of which has increased over the years. The patient reported difficulty seeing in bright light, photophobia, and stated that her vision was better in dark environments. She also had difficulty with colour discrimination and poor distance vision since childhood. Her developmental milestones were appropriate for her age, with no evidence of neuromotor delay.

Ocular findings The patient presented with reduced visual acuity and oscillatory movements in both eyes. Her best corrected visual acuity was 20/200 bilaterally. Colour vision testing with Ishihara plates showed abnormal colour discrimination. She scored 1/21 on the Ishihara test in each eye. Refractive examination revealed myopia and astigmatism in both eyes. Horizontal pendular nystagmus was present bilaterally. Slit-lamp examination of the anterior segment revealed no pathological findings. Fundus examination revealed optic disc pallor and salt-pepper appearance in both the macula and the peripheral retina (Fig. 2a-d). OCT macular scans showed bilateral diffuse retinal thinning with no evidence of subretinal or intraretinal fluid (Fig. 2e, f). VEP testing showed no significant VEP response in the right anterior visual pathway, while latency delays were seen in the left anterior

Table 1 Ophthalmological examinations of the cases

Gene	Type	Nucleotide/protein changes	Age at examination	Congenital nystagmus	Reduced visual acuity	Refractive errors	Photophobia	Reduced or complete lack of color discrimination	Fundus appearance
Case 1 <i>CNGB3</i>	ACHM3	c.739-754del (p.Ala247Thrfs*27) c.1148del(p.Thr383Ilefs*13)	9	+	+	Hyperopia	+	+	Bilateral optic disc pallor, arteriolar attenuation, and bone spicules in the periphery of the major vascular arcs
Case 2 <i>CNGA3</i>	ACHM3	c.1710C>A(p.Ser570Arg)	18	+	+	Myopia	+	+	Bilateral optic disc pallor and salt-pepper appearance both in the macula and peripheral retinal regions
Case 3 <i>CNGA3</i>	ACHM2	c.1710OA(p.Ser570Arg)	15	+	+	Myopia	+	+	Bilateral optic disc pallor and salt-pepper appearance both in the macula and peripheral retinal regions
Case 4 <i>CNCA3</i>	ACHM2	c.1710C>A(p.Ser570Arg)	9	+	+	Hyperopia	+	+	Bilateral optic disc pallor and salt-pepper appearance both in the macula and peripheral retinal regions
Case 5 <i>CNGB3</i>	ACHM2	c.1006G>T(p.Glu336*)	14	+	+	Myopia	+	+	Optic disc pallor temporarily

Table 2 Variants identified in the cases

	Genetic Test	Gene	Variants	Transcript ID	Known/novel variant	Gnom AD frequency	ACMG	Coverage depth
Case 1 (Allele 1)	CES v3	CNGB3	c.1148del (p.Thr- 3831lefs*13)	NM_019098.5	Known Clinvar ID:5225	0.001750	PVS1, PM2	147
Case 1 (Allele 1)	CES v3	CNGB3	c.739-754del (p.Ala247Th- rfs*27)	NM_019098.5	Novel	0	PVS1, PM2	144
Case 2	CES v2	CNGA3	c.l710C>A(p. Ser570Arg)	NM_001298.3	Novel	0	PM1, PM2, PM5, PP3	136
Case 3	CES v2	CNGA3	c.l710C>A(p. Ser570Arg)	NM_001298.3	Novel	0	PM1, PM2, PM5, PP3	156
Case 4	CES v2	CNGA3	c.l710C>A(p. Ser570Arg)	NM_001298.3	Novel	0	PM1, PM2, PM5, PP3	132
Case 5	CES v3	CNGB3	c.l006G>T(p. Glu336*)	NM_019098.5	Known Clinvar ID:188968	0.00004031	PVS1, PM2	95

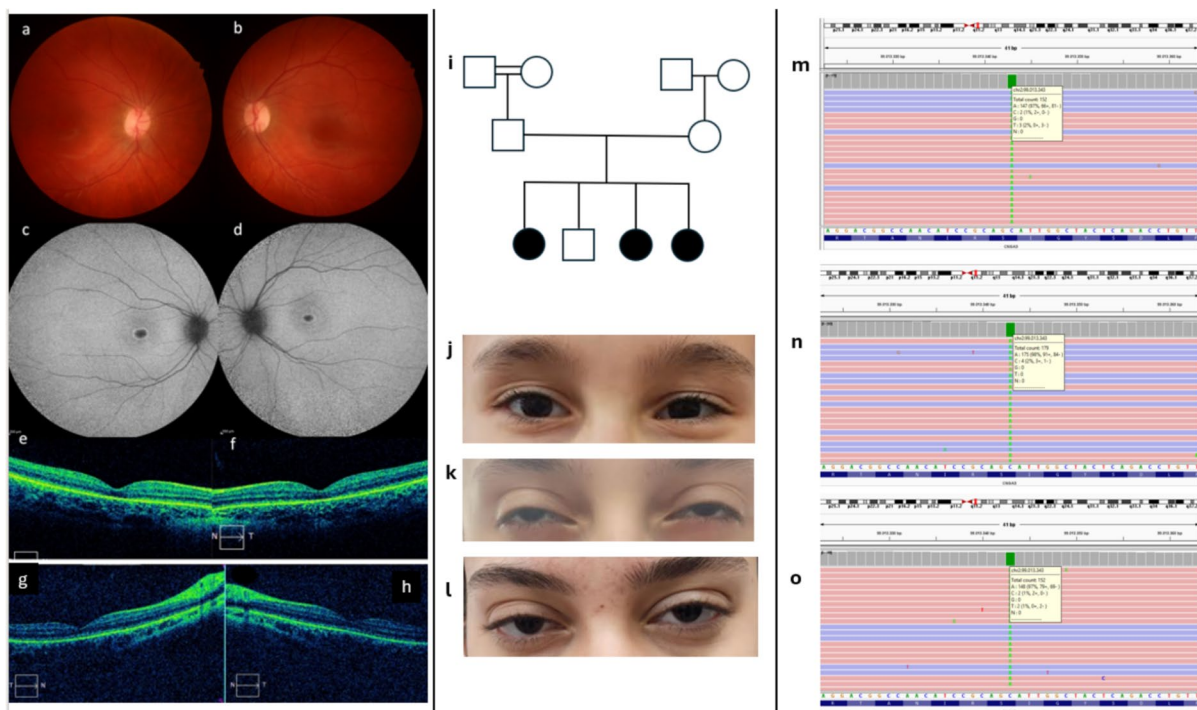


Fig. 2 Bilateral optic disc pallor and salt-and-pepper appearance in case 3 (a and b), bilateral annular hyperautofluorescence representing possible photoreceptor attenuation (c and d), macular OCT scans showing diffuse retinal thinning and loss of normal retinal architecture in the perifoveal region (e and f), macular OCT scans showing diffuse retinal thinning and loss of normal retinal architecture in case 2 (g and h), the

pedigree of Case 2, Case 3 and Case 4 showing the inheritance pattern of the *CNGA3* variant within the family (i), the difficulty in fully opening the eye due to photophobia observed in Case 4 (j), Case 3 (k) and Case 2 (l); and the Integrated Genomics Viewer (IGV) representation of the homozygous novel *CNGA3*: c.l710C>A p.(Ser570Arg) variant in case 2 (m), case 3 (n) and case 4 (o)

visual pathway. ERG showed cone dysfunction with partial rod involvement (Table 1).

Case 4 (C4) She is the 9-year-old sister of C2 (Fig. 2j). Her family noticed bilateral nystagmus at birth. The patient reported difficulty seeing in bright light and photophobia, and groping in brightly lit environments was observed in infancy. She also had difficulty with near vision. Her developmental milestones progressed appropriately for her age with no evidence of neuromotor delay.

Ocular findings The patient presented with reduced visual acuity and oscillatory movements in both eyes. Her best corrected visual acuity was 20/200 in the right eye and 20/400 in the left eye. Colour vision testing with Ishihara plates revealed abnormal colour discrimination. She scored 1/21 in each eye on the Ishihara test. Refractive examination revealed myopia and astigmatism in both eyes. Using the prism and cover test at distance, she had 14 prism diopters (PD) of esotropia in the primary position in the right eye. Horizontal pendular nystagmus was present bilaterally. Slit-lamp examination of the anterior segment revealed no pathological findings. Fundus examination revealed pallor of the optic disc and salt-pepper appearance in both the macula and the peripheral retina. OCT macular scans showed bilateral diffuse retinal thinning with no evidence of subretinal or intraretinal fluid. VEP showed P100 latency in the upper limits in both anterior visual pathways. ERG showed cone dysfunction with partial rod involvement (Table 1).

Genetic analysis identified a homozygous *CNGA3* NM_001298.3:c.1710C>A p.(Ser570Arg) missense variant in all three siblings. Segregation analysis confirmed that both parents were heterozygous carriers of the variant. To the best of the authors' knowledge, this is a novel variant and has not been previously reported in the literature (Fig. 2m–o), (Table 2).

Family 3

Case 5 (C5) A 14-year-old boy was born to healthy Turkish parents who were third cousins. His birth weight and height were within normal limits. The family reported that he initially had a mild motor delay but eventually caught up with his peers. The patient had nystagmus since birth and was referred to an ophthalmologist at the age of 6 months due to a lack of light tracking during a paediatric examination.

A VEP test at the age of 2 years showed delayed and reduced nerve conduction in the visual centre. A repeat VEP test at the age of 4 years showed progression of visual loss. Eye examinations also revealed impaired distance vision. It was noted that the patient had difficulty seeing in bright light, but saw better in the dark. He was also observed to squint in bright environments to reduce light exposure. He had been diagnosed with myopia, nystagmus and photophobia, and the difficulty with colour discrimination was first noted two years ago. There was no family history of a similar condition.

Ocular findings The patient presented with photophobia in both eyes. His best corrected visual acuity was 20/200 in the right eye and 20/400 in the left eye. Colour vision testing with Ishihara plates showed abnormal colour discrimination. He scored 1/21 on the Ishihara test in each eye. Slit-lamp examination of the anterior segment revealed no pathological findings. Fundus examination showed temporal optic disc pallor. Macular OCT scans showed bilateral diffuse retinal thinning with no evidence of subretinal or intraretinal fluid. Retinal nerve fibre analysis showed bilateral marked reduction in mean RNFL thickness (Fig. 3). VEP showed normal responses in both anterior visual pathways. ERG showed cone dysfunction with partial rod involvement (Table 1).

Genetic analysis revealed a homozygous non-sense variant in the *CNGB3* gene: NM_019098.5: c.1006G>T p.(Glu336*). The *CNGB3* c.1006G>T variant has been previously reported in cases of achromatopsia. Segregation analysis confirmed that both parents were heterozygous carriers of the variant (Table 2).

Molecular dynamics studies

Molecular dynamics studies were performed using NAMD 2.0 [17] for 10 ns under NVT conditions. Langevin dynamics was used for temperature control and pulse for the MTS algorithm. All visualisations were performed using the Biovia Discovery Studio program. (BIOVIA, Dassault Systèmes, [Discovery Studio], [2022], San Diego: Dassault Systèmes, [2022]).

In silico studies are theoretical-computational methods used to develop hypotheses about biological phenomena that are difficult to observe. In this study, the 3D structure of the cyclic nucleotide-gated

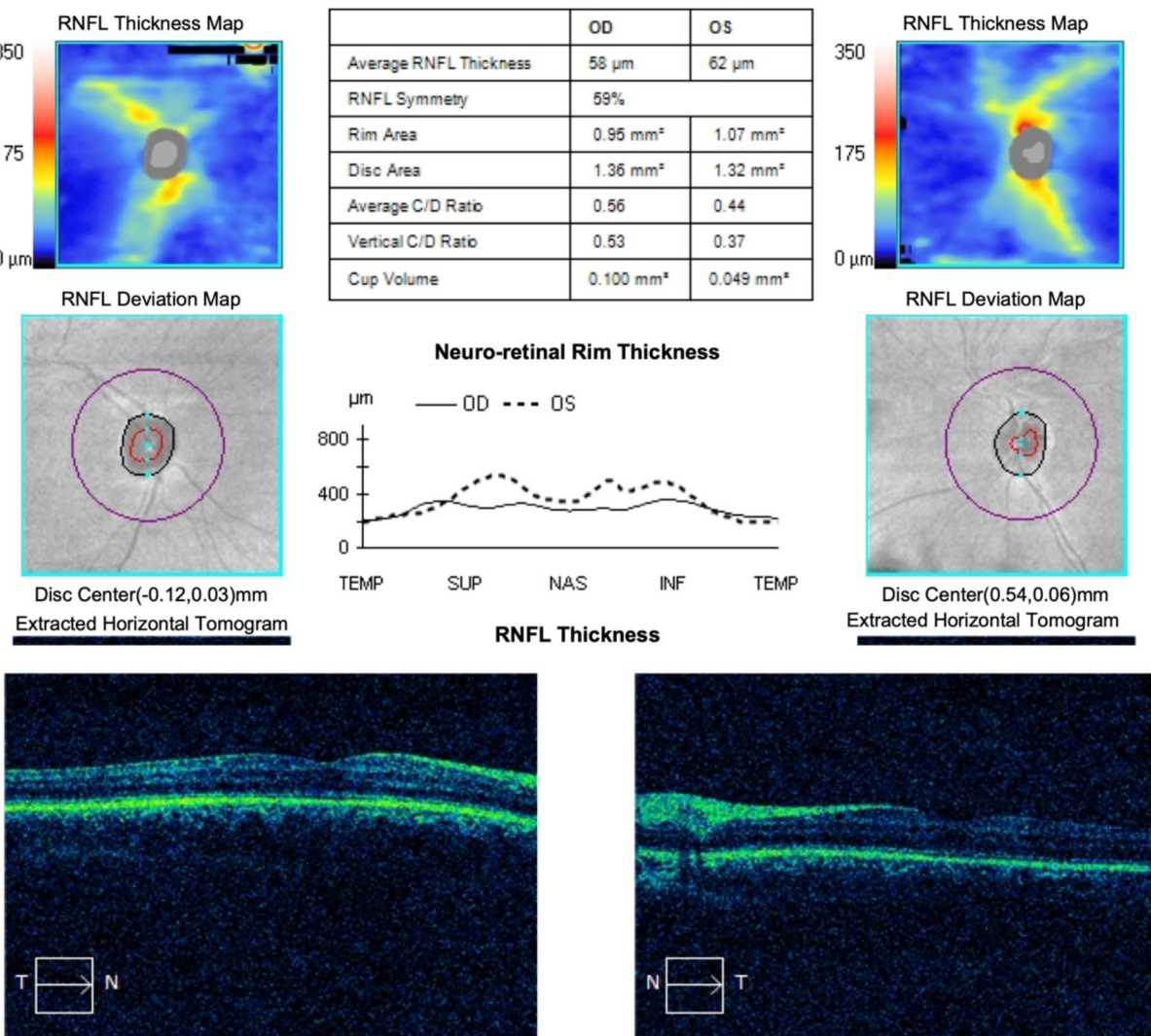


Fig. 3 Structural and functional retinal abnormalities observed in case 5, who carries a homozygous *CNGB3* c.1006G>T p.(Glu336*) nonsense variant. **a** Retinal nerve fibre layer (RNFL) analysis shows significant bilateral thinning, consistent with progressive neuroretinal degeneration. **b** Macular OCT scans show diffuse retinal thinning and disruption of

normal retinal architecture, suggesting cone photoreceptor dysfunction. These findings are consistent with previously reported structural abnormalities in *CNGB3*-associated achromatopsia and highlight the utility of multimodal imaging in characterising disease progression

channel proteins beta-3 and alfa-3 was analysed with different variants using molecular dynamics (MD) methods, and the 3D conformations of the structures formed as a result of the variants were studied. It can be seen that the structures other than the Ser570Arg variant are immature due to the amino acid deficiency. While the conformational energy of the wild-type (WT) structure after MD was found to be -156648.5329 kcal/mol, the energy value of

the Ser570Arg variant structure was found to be -164378.0012 kcal/mol. It is not possible to make such a comparison for other structures in the immature state. However, in structures with other variants, although the protein is in an immature state, changes in the secondary structure are noticeable. It is obvious that these changes occur in order to stabilise the immature structure itself (Fig. 4).

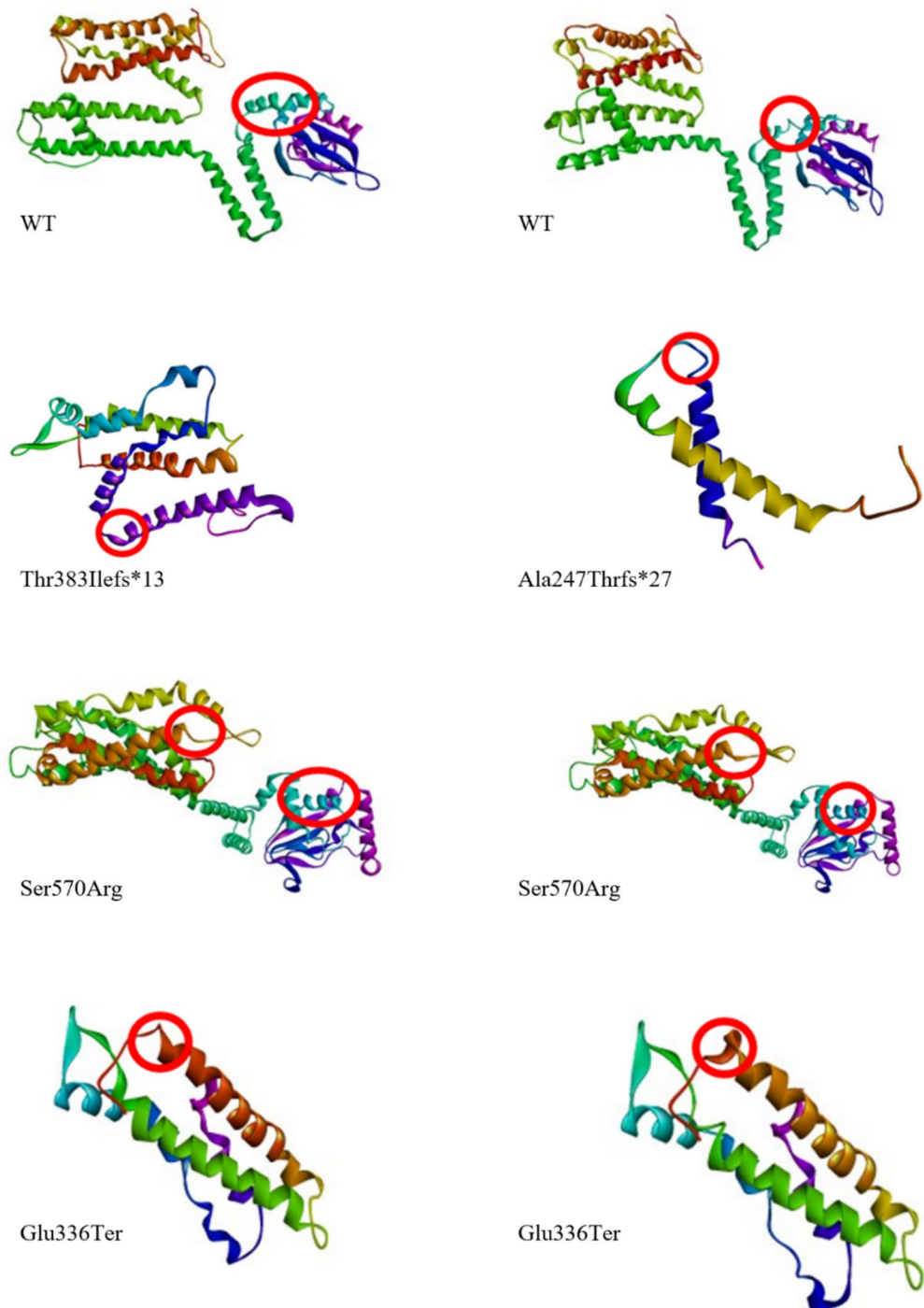


Fig. 4 Secondary structure views of wild type (WT) and other mutant constructs before and after molecular dynamics (MD). Regions marked in red indicate structural changes in the protein after MD

Discussion

In a study of 341 patients with achromatopsia from 10 different countries, *CNGB3* variants were identified in 163 patients. This study showed that *CNGB3* variants are the most common cause of achromatopsia in individuals of European descent [18]. Furthermore, a separate study of 11 families reported the same c.1148del p.(Thr383Ilefs*13) variant in patients from different geographical backgrounds, highlighting its widespread occurrence in different populations [19].

Case 1 was found to be a compound heterozygote for this variant, and a novel frameshift variant identified in this study, *CNGB3* c.739_754del p.(Ala247Thrfs*27). This combination led to a loss of protein function resulting in the clinical presentation of achromatopsia in the patient. Also case 5 was a homozygous carrier of the *CNGB3* c.1006G>T p.(Glu336*) nonsense variant, the pathogenicity of which has already been reported in the literature. Variants in the *CNGB3* are typically nonsense variants, insertions, deletions that cause frameshifts, and splicing variants that disrupt mRNA processing. This process leads to severe structural and functional defects in cone photoreceptors, resulting in the achromatopsia phenotype [2].

Biallelic variants in *CNGA3* have been identified as the most common genetic cause of achromatopsia in Chinese, Israeli and Palestinian patients [20]. The variants observed in *CNGA3* are predominantly missense. In our study, the *CNGA3* c.1710C>A p.(Ser570Arg) homozygous missense variant was detected in three sisters. Several *CNGA3* variants altering the amino acid at position 570 have been described in the literature, all of which have been reported to be pathogenic [21, 22]. However, the variant identified in our study has not been previously described and is considered a novel variant. The pathogenicity of the variant is supported by its high evolutionary conservation, the REVEL score of 0.9 and the clinical findings of our case, which are compatible with achromatopsia.

All five patients in our study presented with congenital nystagmus, reduced visual acuity, photophobia and severe colour vision impairment. OCT showed diffuse retinal thinning in all patients, consistent with previous findings [23, 24]. Importantly, we observed inter-individual variability, particularly

between siblings carrying the same *CNGA3* variant, suggesting that additional genetic or environmental factors may influence phenotype.

Congenital nystagmus is often one of the first symptoms recognised in patients with achromatopsia [25]. Parents often report improved vision in dim light, while bright environments are a challenge. In early childhood, complete colour blindness may go unnoticed as children struggle to express visual problems. In addition, the ability to mimic colours through brightness discrimination may mask the condition until later [20]. In case 1, the family initially reported no colour vision problems, but testing revealed severe impairment. This highlights that early signs can be difficult to detect and underlines the importance of a comprehensive childhood eye examination for early diagnosis, treatment and counselling.

Achromatopsia is classified as complete or incomplete based on the dysfunction of the cone photoreceptors. Visual acuity is generally better in incomplete cases (logMAR 0.6–1.0) than in complete cases (~1.0). In complete achromatopsia, the ERG shows total loss of all three cone types, whereas incomplete cases may show partial or complete cone dysfunction. Although rod function was once thought to be preserved, recent studies suggest a mild to moderate reduction [23, 24]. Similarly, the fundus was previously thought to be normal, but recent evidence shows macular atrophy [23, 24]. In our study, all patients had logMAR ~1.0, indicating severe impairment. Fundus examination showed optic disc pallor in all cases; case 1 also had vascular narrowing and peripheral pigmentation, while cases 2–4 had bilateral salt-and-pepper retinopathy. ERG confirmed cone dysfunction with reduced photopic responses. These findings highlight the variability of fundoscopic changes associated with achromatopsia. ERG imaging showed a significant reduction in photopic response amplitudes in all patients, indicating cone cell dysfunction.

Refractive errors in patients with achromatopsia vary from person to person [26, 27]. In our study, two patients had hyperopia, three had myopia, and astigmatism was present in all patients. Interestingly, we observed remarkable differences in refractive error between three siblings carrying the same homozygous *CNGA3* variant. Although some of this variation may be due to age-related refractive development, it is unlikely to be the sole explanation. The same

phenotypic variability within families was documented in patients with *CNGA3* and *CNGB3* variants, indicating the possible influence of genetic modifiers, epigenetic regulation or environmental factors. Recent studies have shown that individuals carrying identical variants can show significant differences in cone structure, foveal integrity and visual function, even within the same family, further supporting the involvement of modifying mechanisms [28–32]. Although specific genetic modifiers have not yet been conclusively identified in achromatopsia, such variability echoes findings in other inherited retinal disorders, suggesting that additional molecular or environmental inputs may modulate disease expression in monogenic conditions. Further research is warranted to elucidate these influences in achromatopsia.

A 2017 study applied WES to a family in which three out of six siblings had achromatopsia symptoms, confirming previous findings that NGS-based technologies offer greater diagnostic potential than traditional Sanger sequencing or array-based screening for genetically heterogeneous disorders [31]. Although all patients included in this study had a well-defined clinical diagnosis of achromatopsia and harboured pathogenic variants in known associated genes, we chose to use a clinical exome sequencing panel covering a wide range of genes related to inherited retinal diseases. This strategy was chosen for two main reasons. First, the clinical features of retinal dystrophies often overlap, making differential diagnosis based on phenotype alone challenging. Second, the use of a broader panel allows for the detection of additional or unexpected findings, including dual diagnoses or novel gene associations. In this regard, the use of NGS has increased diagnostic confidence and may have broader utility in cases with less typical phenotypes. Thus, while clinical diagnosis in this particular cohort may guide a more targeted testing strategy, our findings do not detract from the value of NGS panels in routine diagnostic workflows for retinal disorders.

One of the key findings of this study is that the Ser570Arg variant has a more negative potential energy value, indicating that the molecule adopts a more stable conformation compared to the WT protein. Previous studies have shown that *CNGA3* and *CNGB3* variants can result in both loss-of-function and gain-of-function effects [33, 34]. While it was expected that the WT protein would retain a higher

stability, the increased stability of the Ser570Arg variant may indicate a potential gain-of-function effect. However, this alone does not indicate a gain of function. If this change causes the channel to pass more ions, to be activated without stimulation, or to stay open longer, it could be a gain of function. However, MD simulations only show structural stability or conformational change, not functional effect. Electrophysiological tests and/or in vitro functional analyses are needed to understand this. Therefore, a more negative energy indicates that the S570R variant makes the protein more stable and possibly folds properly. Clinical evaluation of patients carrying this variant will be crucial to elucidate its phenotypic effects and potential impact on disease progression, and to further refine our understanding of *CNGA3*-associated pathophysiology. In addition, electrophysiological and structural analyses of novel variants, such as S570R, will help us to better understand the molecular mechanisms of achromatopsia [35]. These analyses may provide critical insights for identifying treatment targets and developing new therapeutic strategies. The mutant protein may have a lower energy and possibly a more rigid/stable conformation.

Conclusion

NGS technologies are an important tool in the diagnosis of genetically heterogeneous autosomal recessive disorders, including achromatopsia. The molecular genetic approaches used in this study have provided important insights into the phenotypic effects of *CNGA3* and *CNGB3* variants. In particular, the observation that three siblings carrying the same homozygous *CNGA3* variant had different refractive errors highlights the phenotypic variability associated with achromatopsia.

The identification of two novel *CNGA3* and *CNGB3* variants expands the known genetic spectrum of achromatopsia and deepens our understanding of its pathophysiology. These findings highlight the need for comprehensive genetic screening to improve genotype–phenotype correlations and optimise personalised disease management.

Future studies with larger patient cohorts will be essential to further elucidate genotype–phenotype correlations and optimise clinical interventions. In

addition, functional characterisation of the novel *CNGA3* variant by electrophysiological and structural analyses will further our understanding of the pathophysiology of achromatopsia. An integrated evaluation of genetic and clinical findings is a crucial step towards advancing personalised therapeutic strategies for rare genetic disorders such as achromatopsia.

Acknowledgements The authors thank the families for their cooperation.

Author contributions Z.M.Y. and N.S.F. participated in the design of the study. Z.M.Y., N.S.F., and M.A.U. contributed to the preparation of figures and tables. Z.M.Y., N.S.F., E.E., M.A.U., G.S.V., and E.G. analysed the data and contributed to the interpretation of the data. Z.M.Y., G.S.V. and E.G. revised the article and final approval of the version to be published. All authors read and approved the final manuscript.

Funding No funding is required.

Data availability No datasets were generated or analysed during the current study.

Declarations

Conflict of interest The authors declare that they have no competing interests in this study.

Ethical approval and Consent to participate This study was conducted in accordance with the tenets of the Declaration of Helsinki. Written informed consent for the use of genetic information for research purposes was obtained from patients or their legal guardians who underwent genetic testing at Aydin Adnan Menderes University. As this is a retrospective study, ethical approval was obtained from the Non-Interventional Clinical Research Evaluation Committee of Aydin Adnan Menderes University Faculty of Medicine (protocol number: 2025/67; date: 06.03.2025).

References

1. Kohl S, Jägle H, Wissinger B, Zobor D (2004) Achromatopsia. In: Adam MP, Feldman J, Mirzaa GM, et al. (eds) GeneReviews® [Internet]. University of Washington, Seattle <https://www.ncbi.nlm.nih.gov/books/NBK1418/>
2. Poloschek CM, Kohl S (2010) Achromatopsie. Ophthalmologe 107:571–582. <https://doi.org/10.1007/s00347-010-2178-8>
3. Thiadens AAHJ, Slingerland NWR, Roosing S, van Schooneveld MJ, van Lith-Verhoeven JJC, van Moll-Ramirez N et al (2009) Genetic etiology and clinical consequences of complete and incomplete achromatopsia. Ophthalmology 116:1984–1989. <https://doi.org/10.1016/j.ophtha.2009.03.053>
4. Kohl S, Marx T, Giddings I, Jägle H, Jacobson SG, Apfelstedt-Sylla E et al (1998) Total colourblindness is caused by mutations in the gene encoding the α -subunit of the cone photoreceptor cGMP-gated cation channel. Nat Genet 19:257–259. <https://doi.org/10.1038/935>
5. Kohl S, Baumann B, Broghammer M, Jägle H, Sieving P, Kellner U et al (2000) Mutations in the CNGB3 gene encoding the β -subunit of the cone photoreceptor cGMP-gated channel are responsible for achromatopsia (ACHM3) linked to chromosome 8q21. Hum Mol Genet 9:2107–2116. <https://doi.org/10.1093/hmg/9.14.2107>
6. Kohl S, Baumann B, Rosenberg T, Kellner U, Lorenz B, Vadalà M et al (2002) Mutations in the cone photoreceptor G-protein α -subunit gene GNAT2 in patients with achromatopsia. Am J Hum Genet 71:422–425. <https://doi.org/10.1086/341835>
7. Kohl S, Coppiepers F, Meire F, Schaich S, Roosing S, Brennenstuhl C et al (2012) A nonsense mutation in PDE6H causes autosomal-recessive incomplete achromatopsia. Am J Hum Genet 91:527–532. <https://doi.org/10.1016/j.ajhg.2012.07.006>
8. Kroeger H, Grimsey N, Paxman R, Chiang WC, Plate L, Jones Y et al (2018) The unfolded protein response regulator ATF6 promotes mesodermal differentiation. Sci Signal 11:eaan5785. <https://doi.org/10.1126/scisignal.aan5785>
9. Kaupp UB, Seifert R (2002) Cyclic nucleotide-gated ion channels. Physiol Rev 82:769–824. <https://doi.org/10.1146/annurev.cellbio.19.110701.154854>
10. Michalakis S, Gerhardt M, Rudolph G, Priglinger S, Priglinger C (2022) Achromatopsia: genetics and gene therapy. Mol Diagn Ther 26:51–59. <https://doi.org/10.1007/s40291-021-00565-z>
11. Kang S, Shaikh AG (2017) Acquired pendular nystagmus. J Neurol Sci 375:8–17. <https://doi.org/10.1016/j.jns.2017.01.033>
12. Lewis SD, Mandelbaum J (1943) Achromatopsia: report of three cases. Arch Ophthalmol 30:225–231. <https://doi.org/10.1001/archoph.1943.00880200073008>
13. Simon GJB, Abraham FA, Melamed S (2004) Pingelapese achromatopsia: correlation between paradoxical pupillary response and clinical features. Br J Ophthalmol 88:223–225. <https://doi.org/10.1136/bjo.2003.027284>
14. Thiadens AAHJ, Somervuo V, van den Born LI, Roosing S, van Schooneveld MJ, Kuijpers RWAM et al (2010) Progressive loss of cones in achromatopsia: an imaging study using spectral-domain optical coherence tomography. Invest Ophthalmol Vis Sci 51:5952–5957. <https://doi.org/10.1167/iovs.10-5680>
15. Richards S, Aziz N, Bale S, Bick D, Das S, Gastier-Foster J et al (2015) Standards and guidelines for the interpretation of sequence variants: a joint consensus recommendation of the American college of medical genetics and genomics and the association for molecular pathology. Genet Med 17(5):405–424. <https://doi.org/10.1038/gim.2015.30>
16. Thomas MG, McLean RJ, Kohl S, Sheth V, Gottlob I (2012) Early signs of longitudinal progressive cone

photoreceptor degeneration in achromatopsia. *Br J Ophthalmol* 96:1232–1236. <https://doi.org/10.1136/bjophthalmol-2012-301737>

- 17. Phillips JC, Hardy DJ, Maia JDC, Stone JE, Ribeiro JV, Bernardi RC et al (2020) Scalable molecular dynamics on CPU and GPU architectures with NAMD. *J Chem Phys* 153:044130. <https://doi.org/10.1063/5.0014475>
- 18. Kohl S, Varsanyi B, Antunes GA, Baumann B, Hoyng CB, Jägle H et al (2005) CNGB3 mutations account for 50% of all cases with autosomal recessive achromatopsia. *Eur J Hum Genet* 13:302–308. <https://doi.org/10.1038/sj.ejhg.5201269>
- 19. Thiadens AAHJ, Roosing S, Collin RWJ, van Moll-Ramirez N, van Lith-Verhoeven JJC, van Schooneveld MJ et al (2010) Comprehensive analysis of the achromatopsia genes CNGA3 and CNGB3 in progressive cone dystrophy. *Ophthalmology* 117:825–830.e1. <https://doi.org/10.1016/j.ophtha.2009.09.008>
- 20. Sun W, Zhang Q (2019) Diseases associated with mutations in CNGA3: genotype-phenotype correlation and diagnostic guideline. *Prog Mol Biol Transl Sci* 161:1–27. <https://doi.org/10.1016/bs.pmbts.2018.10.002>
- 21. Genead MA, Fishman GA, Rha J, Dubis AM, Bonci DMO, Dubra A et al (2011) Photoreceptor structure and function in patients with congenital achromatopsia. *Invest Ophthalmol Vis Sci* 52:7298–7308. <https://doi.org/10.1167/iovs.11-7762>
- 22. Solaki M, Baumann B, Reuter P, Andreasson S, Audi I, Ayuso C et al (2022) Comprehensive variant spectrum of the CNGA3 gene in patients affected by achromatopsia. *Hum Mutat* 43:832–858. <https://doi.org/10.1002/humu.24371>
- 23. Aboshiha J, Dubis AM, Carroll J, Hardcastle AJ, Michaelides M (2016) The cone dysfunction syndromes. *Br J Ophthalmol* 100:115–121. <https://doi.org/10.1136/bjophthalmol-2014-306505>
- 24. Maguire J, McKibbin M, Khan K, Kohl S, Ali M, McKeeffry D (2018) CNGB3 mutations cause severe rod dysfunction. *Ophthalmic Genet* 39:108–114. <https://doi.org/10.1080/13816810.2017.1368087>
- 25. Simunovic MP, Moore AT (1998) The cone dystrophies. *Eye (Lond)* 12:553–565. <https://doi.org/10.1038/eye.1998.145>
- 26. Di Iorio V, Karali M, Brunetti-Pierri R, Filippelli M, Di Frusco G, Pizzo M et al (2017) Clinical and genetic evaluation of a cohort of pediatric patients with severe inherited retinal dystrophies. *Genes (Basel)* 8:280. <https://doi.org/10.3390/genes8100280>
- 27. Andersen MKG, Bertelsen M, Grønskov K, Kohl S, Kessel L (2023) Genetic and clinical characterization of Danish achromatopsia patients. *Genes (Basel)* 14:690. <https://doi.org/10.3390/genes14030690>
- 28. Hirji N, Aboshiha J, Georgiou M, Bainbridge J, Michaelides M (2018) Achromatopsia: clinical features, molecular genetics, animal models and therapeutic options. *Ophthalmic Genet* 39:149–157. <https://doi.org/10.1080/13816810.2017.1418389>
- 29. Langlo CS, Erker LR, Parker M, Yang P, Arathoon LR, Ratnam K et al (2022) Adaptive optics retinal imaging in CNGA3-associated achromatopsia: retinal characterization, interocular symmetry, and intrafamilial variability. *Invest Ophthalmol Vis Sci* 63(12):16. <https://doi.org/10.1167/iovs.63.12.16>
- 30. Jinda W, Tongsimai S, Atchaneyasakul L, Suphavilai C, Limwongse C, Shotelersuk V et al (2021) Molecular and clinical characterization of Thai patients with achromatopsia: identification of three novel disease-associated variants in the CNGA3 and CNGB3 genes. *Mol Genet Genomic Med* 9(5):e1656. <https://doi.org/10.1002/mgg3.1656>
- 31. Katta M, Chung DC, Lee W, Weleber RG, Pennesi ME, Carroll J (2023) Longitudinal imaging of the foveal cone mosaic in CNGA3-associated achromatopsia. *Invest Ophthalmol Vis Sci* 64(1):5. <https://doi.org/10.1167/iovs.64.1.5>
- 32. Gupta S, Chaurasia A, Pathak E, Mishra R, Chaudhry VN, Chaudhry P et al (2017) Whole exome sequencing unveils a frameshift mutation in CNGB3 for cone dystrophy. *Medicine (Baltimore)* 96:e7490. <https://doi.org/10.1097/MD.0000000000007490>
- 33. Liu C, Varnum MD (2005) Functional consequences of progressive cone dystrophy-associated mutations in the human cone photoreceptor cyclic nucleotide-gated channel CNGA3 subunit. *Am J Physiol Cell Physiol* 289:C187–198. <https://doi.org/10.1152/ajpcell.00490.2004>
- 34. Dai G, Varnum MD (2013) CNGA3 achromatopsia-associated mutation potentiates the phosphoinositide sensitivity of cone photoreceptor CNG channels by altering intersubunit interactions. *Am J Physiol Cell Physiol* 305:C147–159. <https://doi.org/10.1152/ajpcell.00037.2013>
- 35. Zheng X, Li H, Hu Z, Su D, Yang J (2022) Structural and functional characterization of an achromatopsia-associated mutation in a phototransduction channel. *Commun Biol* 5:190. <https://doi.org/10.1038/s42003-022-03120-6>

Publisher's Note Springer Nature remains neutral with regard to jurisdictional claims in published maps and institutional affiliations.

Springer Nature or its licensor (e.g. a society or other partner) holds exclusive rights to this article under a publishing agreement with the author(s) or other rightsholder(s); author self-archiving of the accepted manuscript version of this article is solely governed by the terms of such publishing agreement and applicable law.